JOURNAL OF GEOPHYSICAL RESEARCH, VOL. 104, NO. B11, PAGES 25,167–25,181, NOVEMBER 10, 1999

A simple parameterization of strain localization in the ductile regime due to grain size reduction: A case study for olivine

Jean Braun

Research School of Earth Sciences, The Asutralian National University, Canberra

Jean Chéry, Alexei Poliakov, David Mainprice, Alain Vauchez, Andrea Tomassi, and Marc Daignières

Institut des Sciences de la Terre, de l'Eau et de l'Espace de Montpellier
CNRS et Université Montpellier II, Montepellier, France

Abstract. We propose a simple parameterization of the transition between dislocation creep and grain-size-sensitive creep under conditions characteristic of the lithospheric mantle and derived from the results of laboratory experiments on olivine-rich rocks. Through numerical modeling and linear stability analysis, we determine the conditions under which this transition takes place and potentially leads to strain localization. We pay particular attention to the effect of cooling rate and strain rate which are likely to be dominant parameters in actively deforming tectonic areas. We conclude that at constant temperature, strain localization can only take place if the rheology of the material is nonlinearly related to grain size; that strain localization is facilitated by syndeformation cooling; that there is only a narrow region in the strain rate versus cooling rate parameter space where localization is likely to take place; and that grain growth inhibits strain localization at fast cooling rates but may lead to "grain growth localization" at low cooling rates. We draw attention to the potential consequences of our analysis of strain localization for the style of plate motions at the Earth's surface.

1. Introduction

Tectonically driven deformation of the lithosphere may lead to strain localization through the formation of frictional faults under low P-T conditions and mylonitic ductile shear zones under high P-T conditions.

Localization in the lithospheric mantle plays a crucial role in determining the style of plate tectonics at the surface of the Earth. Recent three-dimensional models of mantle convection have demonstrated that basic features of plate motion near the surface such as asymmetric subduction zones and oblique (strike-slip) plate boundaries require some sort of rheological weakening to be included in the models [*Zhong and Gurnis,* 1996], such as shear heating [*Bercovici,* 1996] or strain softening [*Tackley,* 1998].

While localization in the brittle regime is relatively well documented [*Paterson,* 1978], the processes of strain localization in the ductile regime (or mylonization) are relatively poorly constrained [e.g., *Poirier,* 1980]. These processes could be associated with a rapid drop in strength (or softening) related to deformation-driven grain size reduction leading possibly to grain-size-sensitive (GSS) creep competing with dislocation creep to become the dominant deformation mechanism [*Poirier,* 1980]. This hypothesis is supported by numerous observations of grain size reduction in strongly deformed lithospheric mantle shear zones [*Vissers et al.,* 1995; *Jin et al.,* 1998].

Stress versus strain rate (or constitutive) relationships have been determined in the laboratory for olivine-rich rocks both in the dislocation and GSS (diffusion) creep regimes [*Karato et al.,* 1986; *Hirth and Kohlstedt,* 1995a,b]. A grain size versus deviatoric stress (or piezometric) relationship has also been clearly established for olivine-rich rocks and appears to hold for a large range of stress, temperature, and water content [*Van der Wal et al.,* 1993; *Twiss,* 1977]. Note that such a piezometric relationship is not unique to olivine-rich rocks [*Twiss,* 1977] and is also commonly observed in other rocks [e.g., *Rutter and Brodie,* 1988], metals [e.g., *Sakai,* 1989] and salt [e.g., *Eggeler and Blum,* 1981].

Our focus here is on combining these relationships in order to develop a formalism (or parameterization) that predicts the evolution and spatial distribution of grain size in an actively deforming system and its effect on

Paper number 1999JB900214.
0148-0227/99/1999JB900214$09.00

rock strength. Our emphasis on grain size is justified because grain size distribution is commonly the main (if not the only) record of strain localization in the ductile regime found in naturally deformed rocks.

The end product of this study is a relatively simple parameterization of strain localization by grain size reduction that can be incorporated in large-scale numerical models of lithospheric deformation and/or mantle flow and, potentially, help to estimate the importance of localization on the style of plates motion at the surface of the Earth.

Attempts at including strain softening by transition from dislocation creep to grain-size-sensitive diffusion creep in numerical models have been ad hoc and only marginaly successful at producing strain localization [*Govers and Wortel,* 1993; *Hopper and Buck,* 1993; *Furlong,* 1993]. More recently, *Kameyama et al.* [1997] have proposed a parameterization very similar to the one developed here. In the present study we go several steps further by (1) clearly defining the conditions under which strain localization is likely to take place in the lithospheric mantle, (2) considering strain localization under constant temperature and constant cooling conditions, and (3) predicting grain size distribution at the end of a synthetic tectonic experiment which can be directly compared to field observations.

2. Formalism

First, we assume that dislocation creep and GSS creep operate independently (ie, the fastest process dominates) [*Langdon and Mohamed,* 1977]. Such an approximation is appropriate to model deformation within a mylonitic shear zone in which planar foliational layers develop parallel to the shearing plane [*Handy,* 1990]. The combined deformation process can be described by an effective viscosity (or ductility) η, given by

$$\frac{2}{\eta} = \left(\frac{1}{\eta_{dl}} + \frac{1}{\eta_{\mathrm{GSS}}}\right), \tag{1}$$

where η_{dl} and η_{GSS} are the viscosities describing the dislocation creep and GSS creep processes, respectively.

Second, we use relatively well-established constitutive relationships derived from high-pressure, high-temperature deformation experiments [e.g., *Karato et al.*, 1986] which describe dislocation and GSS creep of (wet) olivine aggregates. For dislocation creep,

$$\dot{\epsilon} = A_{1,0}\tau^n \exp\left(-\frac{Q_1}{RT}\right) = A_1\tau^n. \tag{2}$$

For GSS creep,

$$\dot{\epsilon} = A_{2,0}\tau d^{-m} \exp\left(-\frac{Q_2}{RT}\right) = A_2\tau d^{-m}. \tag{3}$$

From these, expressions for η_{dl} and η_{GSS} may be derived.

Third, we assume that grain size d tends toward its piezometric value (d_∞, determined by the flow stress value τ) with increasing strain; the simplest formalism that can describe this behavior relates the rate of change of grain size $\dot{d}$ to the deformation rate $\dot{\epsilon}$ according to

$$\dot{d} = -\frac{\dot{\epsilon}}{\epsilon_T}(d - d_\infty), \tag{4}$$

where d_∞ obeys the following piezometric relationship [*Van der Wal et al.,* 1993]:

$$d_\infty = B\tau^{-p}. \tag{5}$$

Because they are generally insensitive to temperature conditions, piezometric relationships have been interpreted [*Van der Wal et al.,* 1993; *Derby and Ashby,* 1987] to be the result of the competition between grain size reduction processes and grain growth. At temperatures characteristic of the lithospheric mantle, grain size reduction takes place by subgrain rotation, grain boundary migration, and/or low-temperature nucleation [*Poirier,* 1980] and is therefore likely to dominate (or at least compete with) grain growth as long as deformation takes place in the dislocation creep regime. For systems deforming in the GSS creep regime, grain growth may become the dominant factor in determining grain size [*Karato,* 1989]. Consequently, the simple relationship (4) is probably only valid when deformation occurs in the dislocation creep regime. In situations where grain reduction processes are inhibited, grain growth proceeds at a rate that is (1) a strong function of temperature and (2) independent of deformation but dependent on the inverse of current grain size. As suggested by *Kameyama et al.* [1997], the transition between dynamic recrystallization in the dislocation creep regime and grain growth only in the GSS creep regime can be parameterized by adding a term to the grain size evolution equation (4) as derived from the experimental work by *Karato* [1989]:

$$\dot{d} = -\frac{\dot{\epsilon}}{\epsilon_T}(d - d_\infty) + \frac{k}{d}\gamma, \tag{6}$$

where

$$k = k_0 \exp\left(-\frac{Q_3}{RT}\right) \tag{7}$$

and

$$\gamma = \frac{\eta_{\mathrm{GSS}}}{\eta_{\mathrm{GSS}} + \eta_{dl}}. \tag{8}$$

The factor γ is introduced to make grain growth the dominant mechanism in the GSS creep regime only. Note that grain size evolution relationships similar to (4) and (6) have been introduced in various modeling and theoretical studies [*Derby and Ashby,* 1987; *Kameyama et al.*, 1997].

In our analysis we first assume that relationship (4) is always valid (this is equivalent to setting $\gamma = 0$ in 6). This simplification permits us to analyze the behavior of our formalism in greater detail by linear perturbation analysis. Later, we evaluate how grain growth can potentially inhibit strain localization near the transition

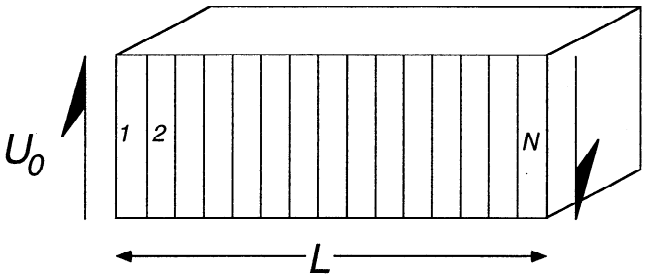

Figure 1. Numerical experiment setup; a volume of rock of length L is sheared at a velocity u_0; the volume is divided into N bands to solve the problem by finite difference.

between dislocation creep and GSS creep by comparing the results of computations performed under the two assumptions: $\gamma = 0$ and $\gamma \neq 0$.

The parameter ϵ_T is a characteristic strain required for the system to approach the recrystallized grain size. It is introduced here to represent the basic behavior of many materials in which the degree of dynamic recrystallization is a function of total accumulated strain.

Laboratory experiments provide only limited information on the amount of strain required for a material to develop a grain size distribution that is directly related to the ambient deviatoric stress value. In metals, strain values of 20 to 100% are necessary to bring the grain size value to the so-called "steady state" structure that is uniquely related to the stress value [*Urcola and Sellars,* 1987; *Sakai,* 1989; *Taplin et al.,* 1979]. In salt, grain size and dislocation density reach steady state value after 3 to 6% transient deformation [*Eggeler and Blum,* 1981]. In Carrara marble, *Rutter* [1995] reports values of 35% strain at 600°C and 20% at 700°C, causing substantial (tens of percents) but not complete recrystallization of the sample. At higher temperature, total dynamic recrystallization can be reached throughout the sample after 30% strain. This critical strain value decreases with increasing temperature. Dynamic recrystallization leading to so-called "foliation weakening" in quartz diorite is observed to develop after 30% strain in coaxial experiments [*Handy,* 1990]. *Rutter and Brodie* [1988] suggest that strain softening that accompanies the transition to GSS creep following dynamic recrystallization in olivine should occur after $\approx$ 40% of permanent natural strain. This estimate is based on the work by *White et al.*[1985] on polycrystalline magnesium. On the basis of a series of deformation experiments on Aheim and Anita Bay dunite samples [*Karato et al.,* 1980, 1982; *Ross et al.,* 1980], *Van der Wal et al.* [1993] report that dynamic recrystallized grain size adjusts to a change of flow stress rather rapidly, provided that enough strain has been achieved (>3% shortening). This rather fragmented information suggests that acceptable values for the parameter ϵ_T in rocks (the only "free" parameter introduced in our formalism) lie between 3 and 40%. There is also a suggestion of a mild temperature dependence [*Rutter,* 1995]. Note that the large range of observed values for ϵ_T may arise from differences between the piezometric grain size and the initial grain size in different experiments.

3. Tectonic Problem

To investigate the behavior of the rheological system described above, we submit it to a simple numerical experiment in which a volume of rock is sheared at a velocity u_0, as shown in Figure 1. This is equivalent to imposing a bulk strain rate, $\dot{\epsilon}_0 = u_0/L$, where L is the arbitrary width of the deforming volume.

Static equilibrium ($\partial\tau/\partial x = 0$, where τ is the shear stress) imposes that the following partial differential equation (PDE):

$$\frac{\partial}{\partial x}\eta\frac{\partial u}{\partial x} = 0; \tag{9}$$

on $u(x)$, the y velocity, must be satisfied everywhere inside the rock. This simplified form of the full three-dimensional static equilibrium equations is based on the assumption that at the onset of localization a strong planar foliation rapidly develops in a direction parallel to the shearing direction such that stress concentration is not permitted [*Handy,* 1990].

This simple PDE, coupled to (1), (4), (2), (3), and (5), can be solved by finite difference. Table 1 gives the values of the various flow parameters used in the numerical experiments. We further assume that as the volume is deforming, it is likely to move toward the Earth's surface and therefore experience cooling at a rate $\dot{T}$.

The width of the volume is discretized in 201(=N+1) nodes (or, equivalently, N bands), and the time evolution of the system is discretized in 10,000 steps. Each band of the volume comprised between two successive nodes is assigned an initial mean grain size, which we refer to as the "grain size" of the band. The grain size

Table 1. Value of Rheological Parameters Used in This Study.

Parameter	Value	Source
B	15 mm $MPa^{4/3}$	1
p	4/3	1
$A_{1,0}$	1.9×10^{3} s^{-1} MPa^{-3}	2
n	3	2
Q_1	420 kJ mol^{-1}	2
$A_{2,0}$	1.5×10^{-3} s^{-1} MPa^{-1} mm^3	2
m	3	2
Q_2	250 kJ mol^{-1}	2
R	8.314 J mol^{-1} K^{-1}	2
k_0	10^{-2} mm^2 s^{-1}	3
Q_3	200 kJ mol^{-1}	3

See text for the meaning of the various symbols.
Sources are (1) *Van der Wal et al.* [1993], (2) *Karato et al.* [1986], and (3) *Kameyama et al.* [1997].

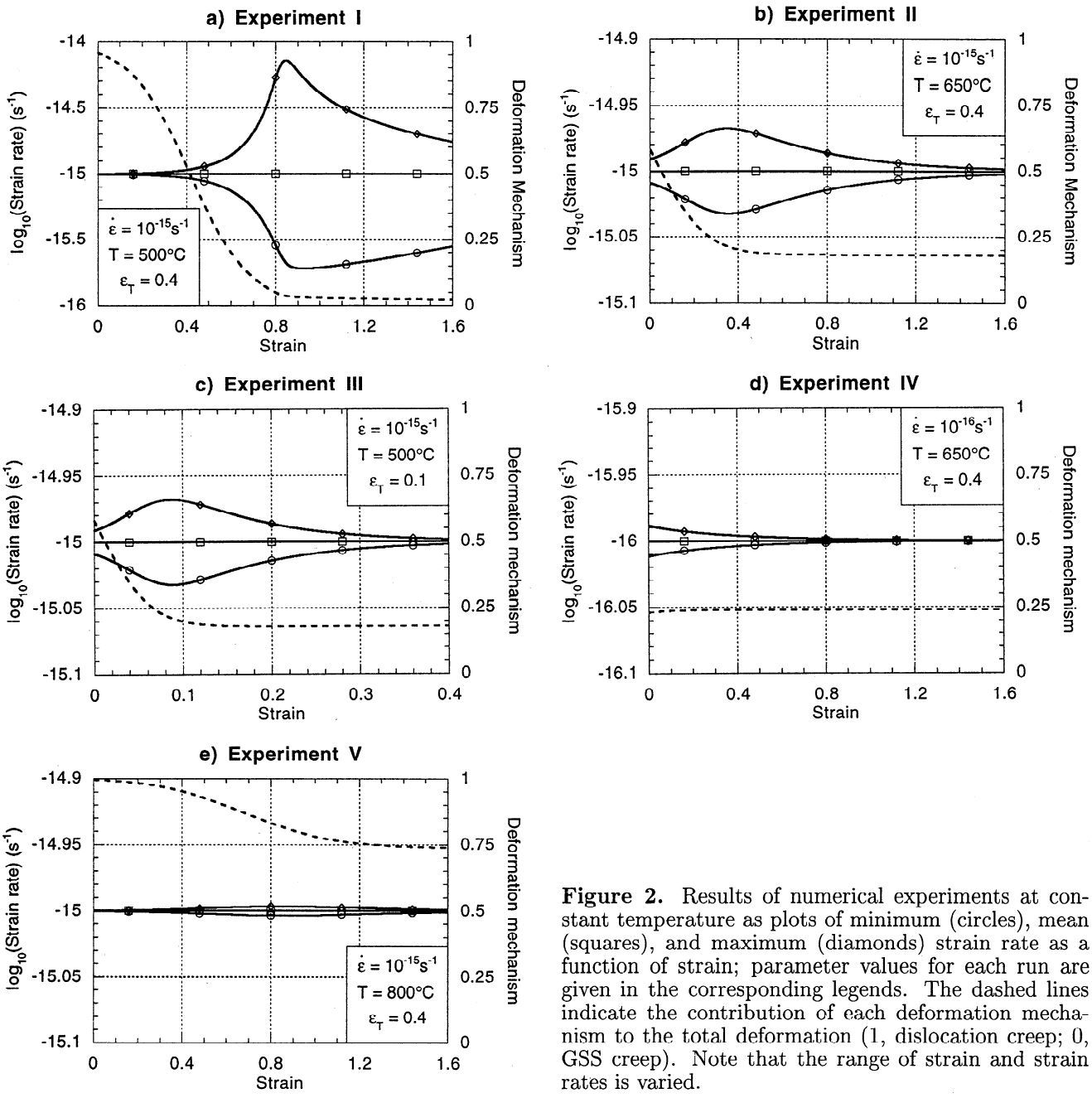

Figure 2. Results of numerical experiments at constant temperature as plots of minimum (circles), mean (squares), and maximum (diamonds) strain rate as a function of strain; parameter values for each run are given in the corresponding legends. The dashed lines indicate the contribution of each deformation mechanism to the total deformation (1, dislocation creep; 0, GSS creep). Note that the range of strain and strain rates is varied.

in each band is allowed to vary in response to changing conditions and according to (4).

Initially, a random grain size distribution is imposed among the bands with a mean value of 1 mm and a maximum deviation of 0.1 mm. Note that the solution does not depend on these values as long as they are "reasonable" for Earth materials.

This setting is quite similar to the numerical experiments undertaken by *Dutruge et al.* [1993] but in which the kinetics of grain size reduction by recrystallization was simulated by a simple grain division process.

It is important to realize here that the experiments are done (1) at constant velocity, (2) at spatially uniform but time-varying stress level and temperature (the stress is derived from the static equilibrium condition, while the temperature is artificially imposed), and (3) at varying grain size and strain rate, both spatially and temporally, as determined within each band by the assumed constitutive relationship and the grain size evolution equation.

4. Constant Temperature Experiments

A large number of numerical experiments were conducted at various temperatures and for various values of the imposed strain rate and the parameter ϵ_T. All experiments were carried out for a total shear strain of 300%. The results of five of these experiments are shown in Figure 2 as plots of the evolution of the average, maximum, and minimum strain rates against accumulated

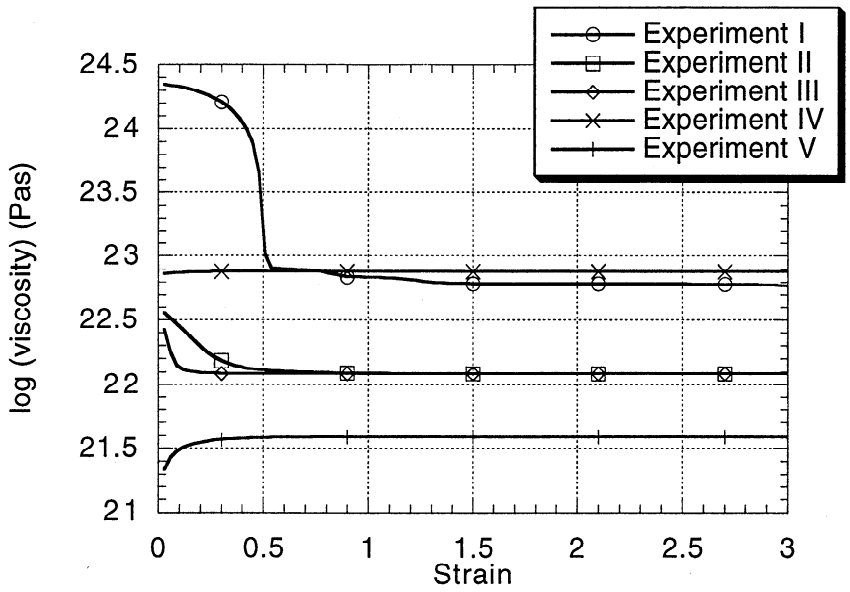

Figure 3. Results of numerical experiments at constant temperature as a comparative plot of viscosity as a function of strain.

deformation. Figure 3 shows the evolution of the mean viscosity (i.e., flow stress τ divided by imposed strain rate $\dot{\epsilon}_0$) of the system with strain.

In all experiments but experiment V, the system has evolved into the GSS creep regime (i.e., GSS creep has become the dominant deformation mechanism). This change of deformation mechanism is accompanied by a reduction in viscosity.

In experiments I, II, and III the system has evolved into localization as, after some finite deformation, the distribution of strain rate in the bands becomes divergent with some bands deforming at very large strain rate and developing very fine grain size, while others stop deforming and are "locked" with relatively large values of the grain size. The localization is also accompanied by a marked reduction in mean viscosity.

The localization is not permanent as, after some deformation, the grain size in the fine grain bands starts to grow back with accumulating strain and the grain size in the coarse grain bands decreases. This phase of grain growth is permitted because even though we are using equation (4) and thus neglect the explicit grain growth term in (6), (1) the piezometric grain size has increased in response to the stress/strength drop associated with the transition to GSS creep and (2) we assume that the system always tries to reach the piezometric grain size which results from the competition between grain growth and grain size reduction processes. Ultimately, all bands are characterized by the same grain size and the localization event is erased from the information contained in the grain size distribution. Note that this reequilibration to a unique grain size is not instantaneous and has not yet been reached in the first experiment after 160% of strain.

This long-term (i.e., large deformation) behavior depends strongly on assumptions we make regarding the grain size evolution beyond the transition to GSS creep. The conditions for localization do not depend on these assumptions as localization takes place while the system is near or at the transition.

To summarize, the results of this first set of computations clearly show that depending on the conditions under which the experiment is conducted and depending on the value of the parameter ϵ_T, the system shows a range of behaviors that includes (1) uniform deformation in the dislocation creep regime (experiment V), (2) uniform deformation in the GSS creep regime (experiment IV), and (3) transient localized deformation after entering the GSS creep regime (experiments I to III). This suggests that although based on a relatively simple formalism, the system is complex and therefore requires better understanding. We propose now to investigate the transition between the dislocation and GSS creep regimes under constant temperature conditions using a simplified linear perturbation analysis.

5. Linear Perturbation Analysis: Part 1

5.1. Transition to Diffusion Creep at Constant Temperature

The transition to GSS creep takes place when the stress level required to accommodate the deformation at the given strain rate and temperature by GSS creep is smaller than the stress level required by dislocation creep.

We assume that the system is deforming in the dislocation creep regime at a flow stress value given by (2):

$$\tau = (\frac{\dot{\epsilon}_0}{A_1})^{\frac{1}{n}}, \tag{10}$$

while the grain size tends towards the piezometric value (5):

$$d_\infty = B\tau^{-p} = B(\frac{\dot{\epsilon}_0}{A_1})^{-\frac{p}{n}}. \tag{11}$$

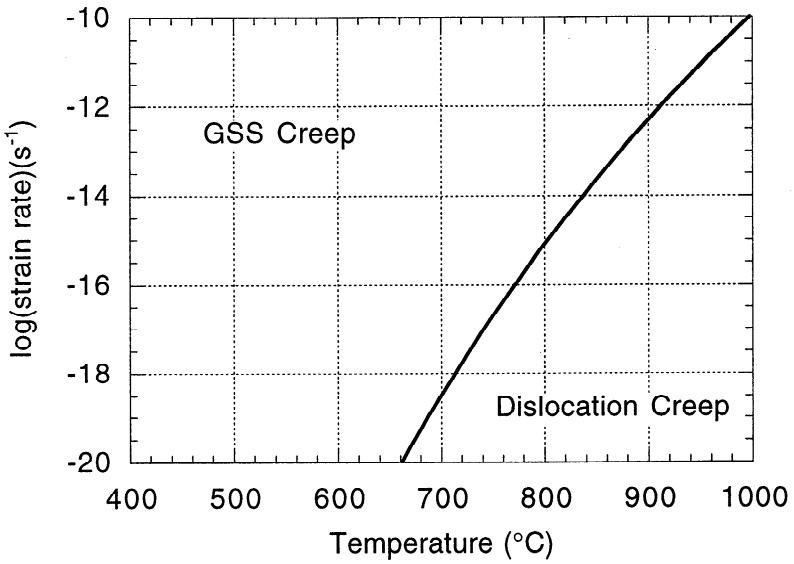

Figure 4. Location in the temperature-strain rate parameter space of the transition between dislocation creep and GSS creep for isothermal deformation as derived from laboratory data for olivine-rich rocks.

Transition into the GSS creep regime will take place when the flow stress value in the GSS creep regime, given by (3)

$$\tau \approx d_\infty^m \left(\frac{\dot{\epsilon}_0}{A_2}\right) = B^m \left(\frac{\dot{\epsilon}_0}{A_1}\right)^{-\frac{pm}{n}} \left(\frac{\dot{\epsilon}_0}{A_2}\right) \tag{12}$$

is smaller than the flow stress value in the dislocation creep regime. This is equivalent to the following inequality representing the conditions for the system to enter the GSS creep regime:

$$\dot{\epsilon}_0^{1+mp-n} > A_1^{1+mp} B^{mn} A_2^{-n}. \tag{13}$$

This relationship is show in Figure 4. Typical Bulk geological strain rates being rarely greater than 10^{-14}s^{-1} suggests that GSS creep can only be an efficient deformation mechanism in the uppermost part of the lithospheric mantle at temperatures lower than 840°C.

5.2. Condition for Localization at Constant Temperature

To derive a condition for localization, we shall assume that at the transition between dislocation and GSS creep, deformation is equally accommodated by the two mechanisms and therefore in each band i the following constitutive relationship applies:

$$\dot{\epsilon}_i = \frac{1}{2} A_1 \tau^n + \frac{1}{2} A_2 \tau d_i^{-m} = A_2 \tau d_i^{-m}, \tag{14}$$

while the piezometric relationship (5) is still valid. This is an approximation that is certainly valid during the transition from dislocation creep to GSS creep, while in each band a nonnegligible proportion of the material is still in the dislocation creep regime.

The grain size in band i can be expressed as

$$d_i = \bar{d} + D_i \tag{15}$$

where $\bar{d}$ is the mean grain size (averaged over all N bands), with the conditions that

$$\sum_{i=1}^{N} D_i = 0 \tag{16}$$

and

$$D_i << \bar{d}. \tag{17}$$

One can show (Appendix A) that the mean grain size $\bar{d}$ obeys the following evolution equation:

$$\dot{\bar{d}} = -\frac{\dot{\epsilon}_0}{\epsilon_T}(\bar{d} - d_\infty), \tag{18}$$

whereas the deviation from the mean grain size in band i, D_i, obeys (Appendix A)

$$\dot{D}_i = -\frac{\dot{\epsilon}_0}{\epsilon_T} D_i [1 - m(1 - \frac{d_\infty}{\bar{d}})]. \tag{19}$$

The solution of (19) is quite complex, as d_∞ is a function of the flow stress and hence of time. However, one can easily see that it takes the form of a growing exponential in situations where

$$1 - m(1 - \frac{d_\infty}{\bar{d}}) < 0 \tag{20}$$

or

$$\bar{d} > \frac{m}{m-1} d_\infty, \tag{21}$$

which leads to a rapid decrease in grain size ($\dot{D}_i < 0$) in the bands characterized by a grain size smaller than the mean ($D_i < 0$) and an equally rapid increase in grain size ($\dot{D}_i > 0$) in the bands characterized by a grain size larger than the mean ($D_i > 0$). This explosion in grain

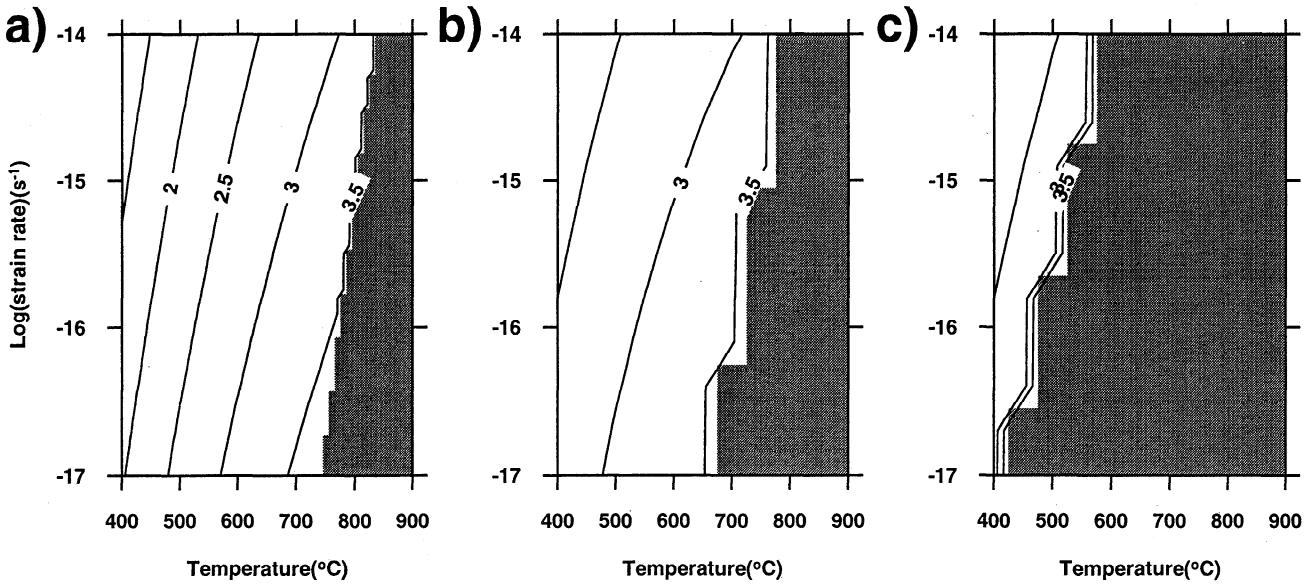

Figure 5. (a) Contour plot of the logarithm of the minimum grain size required for localization during deformation at constant temperature; the shaded area corresponds to the region of the parameter space where dislocation creep is more efficient than GSS creep at accommodating deformation; (b) computed grain size at the onset of localization assuming that equation (4) is always valid ($\epsilon_T = 0.4$ in all experiments); (c) same as Figure 5b but assuming that equation (6) determines the evolution of grain size.

size away from the mean value leads to an increase in strain rate (and thus localization) in the bands where the grain size decreases exponentially and a decrease in strain rate in the bands where the grain size increases exponentially.

Equation (21) may be rewritten as

$$\bar{d} > [\frac{m}{m-1} B (\frac{A_2}{\dot{\epsilon}_0})^p]^{\frac{1}{1+mp}}, \qquad (22)$$

which can be used as a criterion for localization based on the mean grain size of a volume of rock undergoing deformation at an imposed strain rate $\dot{\epsilon}_0$ and at a temperature T (which will determine the value of the parameter A_2).

Physically, this condition (21) states that when the system is at the transition between the dislocation creep and GSS creep regimes, the mean grain size must be substantially greater than the piezometric value for localization to take place. The condition is dependent on the grain size exponent in the GSS creep constitutive relationship m. This implies that the condition for localization is more likely to be fulfilled in highly nonlinear systems ($m > 1$) as $m/m-1$ then tends toward unity; but it cannot be fulfilled if the GSS rheology is linearly dependent on the grain size ($m = 1$). This result is in agreement with the "minimum" condition for localization expressed by *Jin et al.* [1998] that the grain size at the transition from dislocation creep to GSS creep must be greater than the piezometric value at the corresponding stress level. This condition for localization, combined with condition (13) for transition to GSS creep, is shown graphically on Figure 5a as a contour plot of the minimum mean grain size required for localization during the transition to GSS creep. Figure 5b shows contours of the mean grain size at the time of onset of strain localization computed from a large number of numerical model runs in which strain rate and temperature were systematically varied from 10^{-17} to 10^{-17}s^{-1} and 400 to 900°C, respectively. Comparing Figures 5a and 5b demonstrates the agreement between the results of the linear stability analysis and the numerical model. Differences arise from (1) the initial grain size distribution assumed in the numerical model and (2) the definition of 'strain localization' in the numerical model. Two important points must be stressed:

1. Equation (18) indicates that the asymptotic value (at $t = \infty$) for the mean grain size ($\bar{d} = d_\infty$) does not satisfy the condition for localization (21), which implies that localization at constant temperature is always transient: as time evolves (or more exactly as strain accumulates), $\bar{d}$ will ultimately always fall below the critical value for localization; note that this result is dependent on the assumed behavior for the grain size evolution during finite deformation in the GSS creep regime;

2. the condition for localization does not depend on the value of the constant ϵ_T.

6. Cooling Experiments

The results of an experiment in which the rock volume is forced to cool from 1350°C to 400°C at a rate of 10^{-12} °C s^{-1} are shown in Figure 6 as plots of the min-

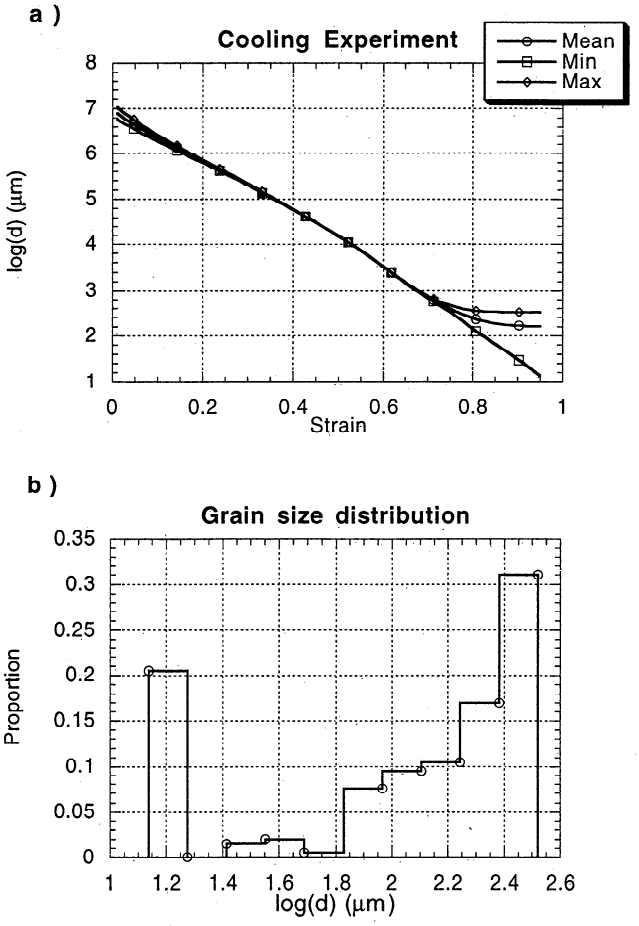

Figure 6. Results of a numerical experiment at constant cooling rate (see text for parameter values); (a) evolution of the minimum, mean, and maximum grain size with strain and (b) final grain size distribution.

imum, maximum, and average grain sizes in the volume as well as the final grain size distribution. The strain rate is fixed at 10^{-15} s^{-1} and $\epsilon_T = 0.05$. The total strain at the end of the experiment is 95%.

Note that the unrealistically large values of the grain size computed at high temperatures are an artifact of using the piezometric relationship (4) in a range of flow stress values at which it is not applicable. This has no effect on the grain size evolution during the transition to GSS creep which takes place at relatively low temperatures under stress conditions at which the piezometric relationship is well constrained.

For these values of the strain rate, cooling rate, and ϵ_T the experiment evolves into localization after 68% of deformation at a temperature of 700°C (Figure 6a). At this point, only a small proportion of the bands continues to experience grain size reduction and accommodates most of the deformation. At the same time, the other bands are abandonned and due to the lack of deformation are frozen at a relatively large grain size.

The final grain size distribution (Figure 6b) shows that at the end of the experiment, only 20% of the bands are still deforming and are characterized by a grain size of 15 μm, while the rest have been abandonned at various grain sizes ranging from a few tens of microns to nearly 1 mm. At the end of the experiment the flow stress is 180 MPa, while the coarse grain bands have stopped deforming at a stress level of 20 MPa.

Changing the parameters and physical conditions of the experiment leads again to a variety of behaviors including (1) deformation in the dislocation creep during the entire experiment, (2) transition to GSS creep without localization, (3) transition to GSS creep that leads to transient localization, and (4) transition to GSS creep that leads to permanent localization.

We also conducted a series of experiments during which the temperature was allowed to increase during deformation; in this situation, regardless of the value of the heating rate, deformation did not lead to localization. Furthermore, in other experiments where the temperature was allowed to vary periodically with time, deformation was always uniform when the temperature was increasing even in situations where strain localization took place during the cooling part of the imposed temperature cycles.

To understand this range of behavior we now generalize the conditions for transition to GSS creep and localization at constant temperature derived from the linear stability analysis to conditions of changing temperature.

7. Linear Stability Analysis: Part 2

7.1. Transition to Diffusion Creep During Cooling

Because the piezometric grain size value decreases with increasing stress, and thus with decreasing temperature, an additional condition arises for the transition from dislocation to GSS creep in the case of a cooling system. For large values of the cooling rate it is possible that the rate of change of the piezometric grain size with deformation (and thus time) is too large for the grain size to ever reach the piezometric value.

The condition on cooling rate for the transition toward GSS creep in a cooling environment can be expressed as (Appendix B)

$$|\dot{T}| < \frac{\dot{\epsilon}_0}{\epsilon_T}\frac{RT^2}{Q_1}\frac{n}{p}. \tag{23}$$

This leads to a new condition on the strain rate for the transition from dislocation to GSS creep (Appendix B); i.e., (13) becomes

$$\dot{\epsilon}_0^{1+mp-n} > A_1^{1+mp} B^{mn} A_2^{-n} \left(\frac{1}{1+\alpha}\right)^{mn}, \tag{24}$$

where

$$\alpha = \frac{Q_1}{RT^2}\dot{T}\frac{p}{n}\frac{\epsilon_T}{\dot{\epsilon}_0}. \tag{25}$$

This relationship is shown in Figure 7. Again, assuming that bulk geological strain rates never excede

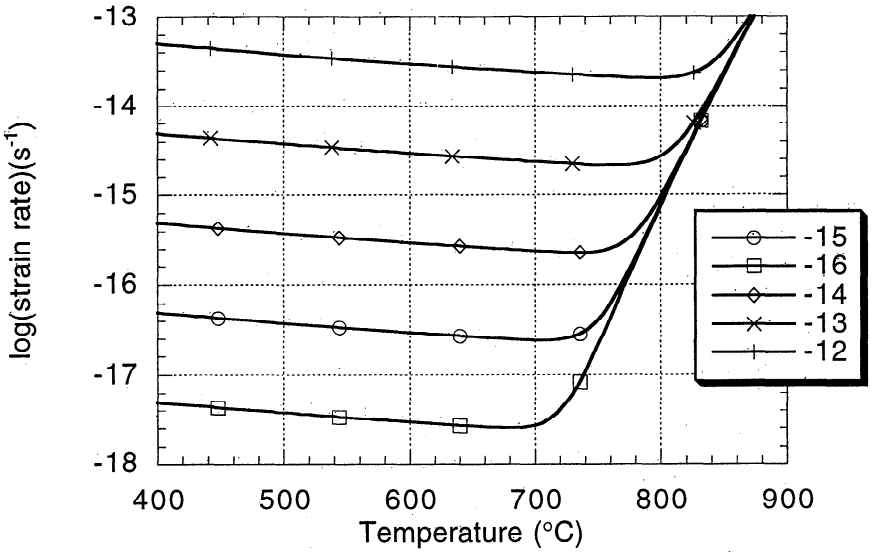

Figure 7. Location in the temperature-strain rate parameter space of the transition between dislocation creep and GSS creep for a range of cooling rate as derived from laboratory data for olivine-rich rocks.

10^{-14} s^{-1} implies that GSS creep can only be an efficient deformation mechanism at temperatures lower than 840°C and for cooling rate lower than 10^{-11} °C s^{-1} ($\approx$ 300°C Myr^{-1}). This estimate is based on an assumed value of 0.1 for ϵ_T; for smaller values of ϵ_T this estimate of the maximum cooling rate is larger and vice versa.

7.2. Condition for Localization During Cooling

The condition for localization is still determined by the behavior of (19) in which d_∞ (the piezometric grain size) varies exponentially with temperature, thus with time, thus with deformation.

The condition for localization becomes (Appendix C)

$$\bar{d} > [\frac{m}{m-1-\kappa} B(\frac{A_2}{\dot{\epsilon}_0})^p]^{\frac{1}{1+mp}}. \quad (26)$$

Using (5) and (A3), one can write

$$d_\infty = B(\frac{A_2}{\dot{\epsilon}_0})^p \bar{d}^{-mp}, \quad (27)$$

and (26) becomes

$$\bar{d} > (\frac{m}{m-1-\kappa}) d_\infty, \quad (28)$$

where

$$\kappa = \frac{Q_2}{RT^2} \dot{T} \frac{\epsilon_T}{\dot{\epsilon}_0} \cdot \frac{p}{1+mp} \quad (29)$$

Because κ is always negative during cooling experiments, (28) clearly shows that cooling makes the condition for localization less stringent; it is even possible to drive a material which has a linear grain size dependence ($m = 1$) into localization by cooling it during deformation.

Unlike in the constant temperature case, localization during cooling can lead to permanent localization. One can easily derive (Appendix C) the condition for the localization to be permanent:

$$|\dot{T}| > \frac{RT^2}{Q_2} \frac{\dot{\epsilon}_0}{\epsilon_T} \frac{1+mp}{p(1+m)}. \quad (30)$$

Note that this relationship is dependent on the assumed grain size evolution "rule" for large deformation in the GSS creep regime.

7.3. Verification of Linear Perturbation Analysis Results

To verify the validity of the predictions of the linear stability analysis, we conducted a large number (16,000) of numerical experiments in which the strain rate, the cooling rate, and the parameter ϵ_T were varied systematically. In all experiments the volume of rock that underwent deformation and cooling was forced to cool from 1350°C to 400°C at the set rate. Note that the results obtained were independent of the starting temperature as long as it was above 850°C. For each experiment we calculated, at each time step, the ratio of the maximum and minimum strain rates among the 201 bands. When that ratio was ¿ 10, we considered that the experiment had led to localization, and we recorded the temperature at which it happened. If it did not, the recorded temperature was arbitrarily set to 400°C.

The results are shown in Figure 8a in which the localization temperature is plotted as a function of the strain rate $\dot{\epsilon}_0$ and the product of the cooling rate $|\dot{T}|$ by the constant ϵ_T. Figure 8a clearly shows that there is only a narrow region in the $[\dot{\epsilon}_0, |\dot{T}|\epsilon_T]$ space in which localization takes place. It follows a straight line in log-log coordinates that can be approximated by

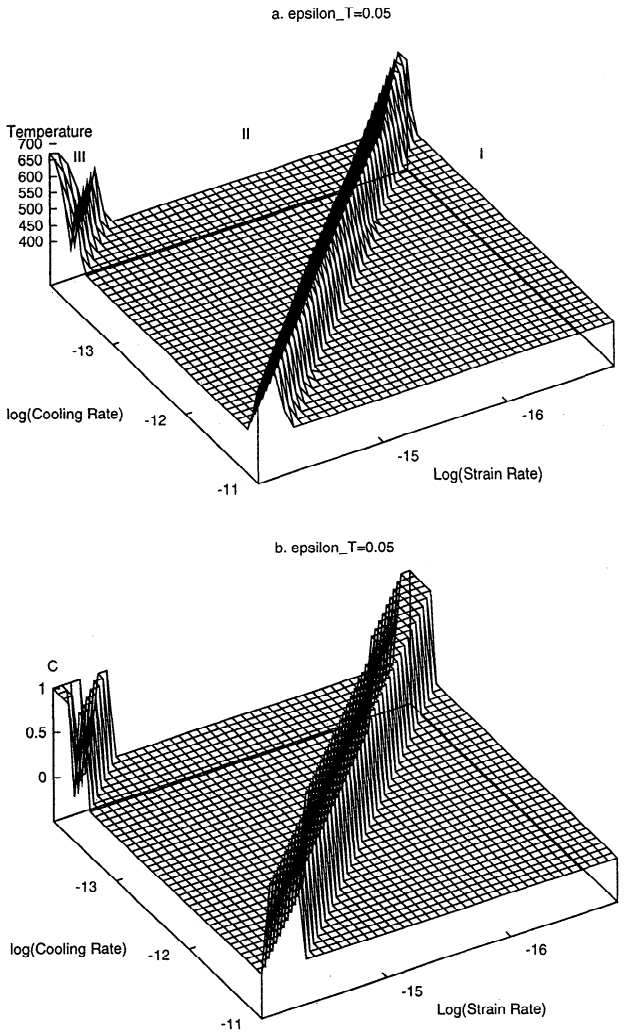

Figure 8. Perspective plot of the temperature at which localization takes place as a function of imposed strain rate and cooling rate; where the temperature is set at 400°C, no localization took place during the numerical experiment. See text for description of regions I, II, and III.

$$\log_{10} \dot{\epsilon}_0 = \log_{10} |\dot{T}|\epsilon_T - 1.7. \qquad (31)$$

We also note in Figure 8a that the temperature at which localization takes place is inversely proportional to both the strain rate and the cooling rate.

In each experiment we also calculated whether the condition for the transition into GSS creep (23) and (24) and the condition for localization (28) were satisfied. When both conditions were satisfied, a parameter C was set to one; when either of the two conditions (or both) was (were) not met, the parameter C was set to zero. In Figure 8b we show the variation of this parameter C in the $[\dot{\epsilon}_0, |\dot{T}|\epsilon_T]$ space. The region of the space where it is equal to 1 is similar to the region of the space where localization takes place, confirming that the conditions for localization derived from the linear perturbation analysis are fully applicable to the nonlinear situation too.

The region of the $[\dot{\epsilon}_0, |\dot{T}|\epsilon_T]$ space marked I in Figure 8a corresponds to situations in which the cooling rate is too large (in comparison with the assumed strain rate) for the system to ever reach the GSS creep regime. The region of the $[\dot{\epsilon}_0, |\dot{T}|\epsilon_T]$ space marked II in Figure 8a corresponds to situations where the strain rate is too large and thus the shear stress is too high, and thus the mean grain size is too low (at the time of transition to GSS creep) for localization to take place.

At low cooling rate and high strain rate the factor κ defined in (29) becomes much smaller than unity and the condition for stability (28) reverts to the condition for stability in the isothermal state (21). This explains the existence of localizing experiments in the [high strain rate, low cooling rate] region (marked III) of the diagram in Figure 8a.

8. Final Grain Size Distribution

In nature, grain size distribution is the main record of localization in the ductile regime. To compare directly the results of our parameterization to natural examples of localization, we present the predicted grain size distribution in four numerical experiments carried out at various strain rates but for which the cooling rate was set to a value leading to localization, i.e., using (31). The results are shown in Figure 9.

All experiments predict the following grain size distribution: (1) a family of very fine grain bands which have deformed in the GSS creep regime since the localization initiated and accommodates all the deformation at the end of the experiment, (2) another family of much coarser grain bands which have experienced little (if any) deformation in the GSS creep regime, and (3) a third family of bands of intermediate grain size, the distribution of which is skewed towards the larger grain size; these intermediary bands have formed after the transition to GSS creep but have been abandonned at various stages since the initiation of localization.

The final mean grain size is inversely proportional to the strain rate (and cooling rate); the ratio of grain sizes in the large grain bands (the "undeformed matrix") and the small grain bands (the "mylonites") is also inversely proportional to the strain rate. The proportion of the bands that are in the large grain size fraction (and thus remain relatively undeformed) is also inversely proportional to the strain rate.

The grain size in the fine grain bands is determined by the stress value at the end of the experiment. The grain size in the large grain bands is determined by the stress value at the time of the transition into GSS creep.

Caution should be taken, however, before grain size distributions derived from observations of naturally deformed mantle peridotites are compared to the predictions of our simplified one-dimensional numerical model. The numerical model is based on the assumption that the deforming shear zone is made of perfectly decoupled (i.e., independent) layers; such an idealized

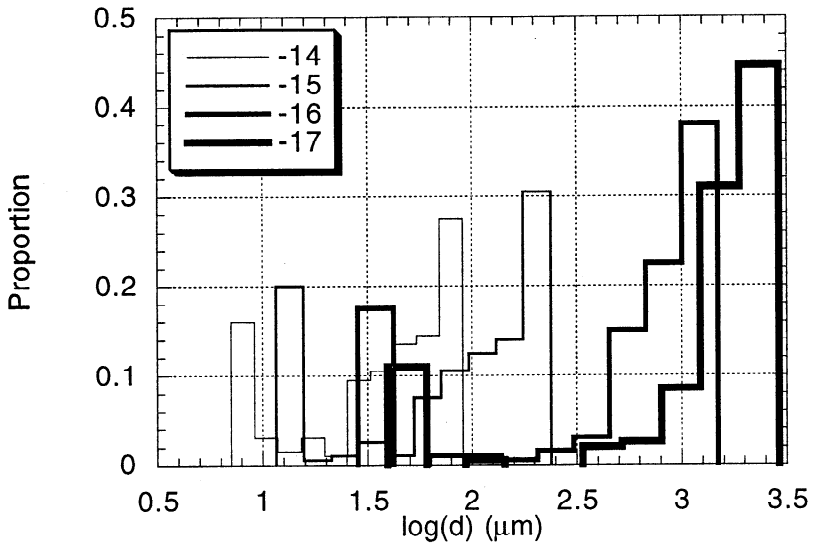

Figure 9. Final grain size distribution for a series of numerical experiments conducted at various strain rates and cooling rates; the strain rate values are indicated in the legend; the cooling rates are chosen to fall within the values necessary for localization as shown in Figure 8.

geometry can only be encountered in nature in situations where a strong foliation has developed in the direction parallel to the shearing direction and stress is therefore quasi-uniform across the structure [*Handy*, 1990].

9. Grain growth

As stated in section 2, there is evidence [*Karato*, 1989] that in olivine, once GSS creep becomes the dominant deformation mechanism, grain growth may dominate dynamic recrystallization in determining grain size (i.e., grain size reduction processes are inhibited).

We have intentionally neglected to incorporate this process in our formulation so far for two reasons: (1) because it is still unclear under what exact conditions grain size reduction processes are inhibited during the transition to GSS creep, we find it difficult to include it in our parameterization which we wish to remain simple, and (2) it is always more instructive to study a complex system by emphasizing its basic behavior and, in a second step, assessing how this behavior is affected by secondary, less well documented, processes.

To investigate the potential effect of such a simplification on our results, we performed a series of numerical experiments at constant temperature in which equation (6) was used to determine the grain size evolution. The results of these experiments are summarized in Figure 5c and should be compared to the equivalent model results performed with equation (4) and shown in Figure 5b. The main difference is an inhibition of localization at high temperatures. This is because grain growth is a thermally activated process. This result is in agreement with the conclusion of *Kameyama et al.* [1997] that grain growth has a stabilizing effect on the development of shear zones during the transition from dislocation to GSS creep even, as their analysis showed, in the presence of viscous heating.

We also performed a series of experiments under constant cooling conditions, similar to those shown in Figure 7 but with equation (6) used instead of (4). The results are shown in Figure 10a and clearly demonstrate that localization is inhibited by grain growth but not prevented. In other words, localization takes place for a similar range of values of cooling rate and strain rate but at lower temperatures than when equation (6) is used to describe grain size evolution.

More interestingly, localization has appeared in a separate region of the $[\dot{\epsilon}_0, |\dot{T}|\epsilon_T]$ parameter space. This regions corresponds to a regime in which grain growth is the dominant mechanism in determining grain size during and after the transition to GSS creep. This could be called "strain localization by grain growth."

As shown in Appendix D, this new localization regime can be constrained to be in regions of the parameter space where

$$|\dot{T}| < \frac{2kRT^2}{\bar{d}^2 Q_3}. \tag{32}$$

Physically, this means that localization may result from selective strengthening of parts of the system by grain growth (which are driven back into the dislocation creep regime) and, subsequently, relative weakening of the remaining parts. In this situation the onset of localization depends on our assumption that the system is forced to deform at a given strain rate.

Several other formulations could be envisaged to incorporate grain growth in a model for grain size evolution in a deforming rock volume. We have performed a series of model runs at constant cooling rate under the assumption that (1) grain growth becomes important when the grain size is smaller than the piezometric value (for the current stress level) and (2) grain growth

is always competing with dynamic recrystallization, i.e., $\gamma = 1$ always. The results of these two series of model runs are shown in Figures 10b and 10c, respectively. Under the first assumption the solution is very similar to the one obtained by neglecting grain growth; under the second assumption the localization can only take place by grain growth, at relatively low cooling rates, as determined by (32).

It is also interesting to note that recent laboratory investigations [*Beeman and Kohlstedt,* 1993] have brought new evidence that there may be a region within the dislocation creep regime where the flow law becomes slightly grain size sensitive. This region lies near the transition to diffusion creep and corresponds to a transition from dislocation creep by slip along the stronger [c] slip system to the weaker [a] slip system [*Hirth and Kohlstedt,* 1995b; *Drury and Fitzgerald,* 1998]. This certainly warrants further investigation and possible incorporation in models of the type described here.

Recent work by *De Bresser et al.*[1998] led to the hypothesis that dynamic recrystallization may represent a balance between grain growth and grain size reduction processes that occurs exactly at the boundary between dislocation creep and GSS creep. In such a situation the piezometric relationship is defined by the grain size value at which both deformation mechanisms accommodate deformation at the same stress value. As shown by *De Bresser et al.*[1998], this hypothesis leads to a temperature dependence of the recrystallized grain size. We have tested the consequences of this hypothesis on the onset of localization by transition to GSS creep in olivine by replacing the piezometric relationship (5) with the equivalent temperature-dependent stress-grain size relationship derived by *De Bresser et al.*[1998]. A new set of numerical experiments exploring the $[\dot{\epsilon}, \dot{T}]$ space showed that under the hypothesis put forward by *De Bresser et al.*[1998], localization is not possible for any of the parameter values investigated.

10. Conclusions and Discussion

We have presented a new formalism to parameterize the transition between dislocation creep and GSS creep in olivine-rich rocks in conditions characteristic of the lithospheric mantle. From this formalism we have derived a series of inequalities (13), (21), (24), (28), and (32) that define the physical conditions and parameter values for which the transition can occur and potentially lead to localization at constant temperature or during constant cooling.

These inequalities provide relatively tight constraints on the range of physical conditions under which localization in the GSS creep regime can take place. In particular, we show that (1) localization at constant temperature is favoured for rheological laws where grain size sensitivity is highly non-linear, (2) localization at constant temperature is not possible in rocks where the grain size dependence of the rheology is linear, (3) localization at constant temperature can only be transient,

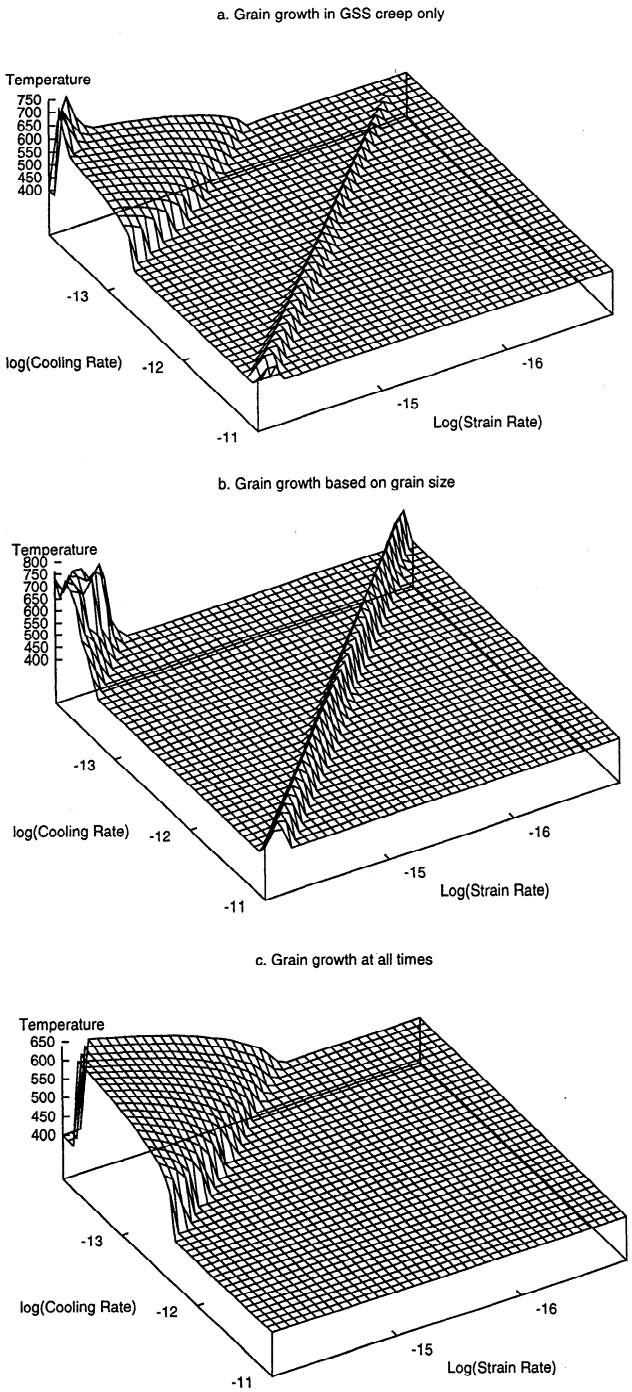

Figure 10. Effect of grain growth on strain localization in a cooling environment; (a) assuming grain growth is dominant in the GSS creep regime only; (b) assuming grain growth is dominant when $d_i < d_\infty$ only; and (c) assuming grain growth is activated in all situations.

(4) localization is more likely to take place during cooling, (5) localization can be triggered in a linear GSS material if deformation is coeval with cooling, and (6) localization in a cooling environment may lead to permanent localization.

Note that cooling leads to permanent localization because it results in an increase in flow stress with time (and deformation) which, in turn, causes smaller grain sizes to develop in accordance with equation (5) in

the actively deforming shear bands. Scenarios could thus be envisaged in which permanent strain localization caused by stress buildup (such as in the early stages of an orogeny) develops in an isothermal environment.

The grain size distributions predicted by our new parameterization can also be used to constrain the conditions under which naturally formed mylonitic shear zones have developed by comparing them to field observations. This requires, however, that the various flow law parameters used in this study be known with reasonable confidence.

Grain growth inhibits localization by dynamic recrystallization but permits a new type of localization (which we call strain localization by grain growth) at relatively low cooling rate.

It is interesting to note that the results of our numerical model (based on the results of laboratory experiments on rock rheology) suggest that the localization conditions are encountered in the Earth's lithosphere. If we consider a tectonically active region subjected to horizontal shortening at a rate $\dot{\epsilon}_0$, in which an equilibrium has been reached between accretion and denudation, the cooling rate of rock particles exhumed at the surface of the orogen can be related (to first order) to the strain rate by

$$|\dot{T}| \approx \dot{\epsilon}_0 \Delta T, \tag{33}$$

where ΔT is the temperature difference between the base of the deforming layer and the surface. Combining this simple relationship with the relationship between cooling rate and strain rate which determines the conditions for strain localization in a cooling environment (31) leads to a condition for localization at the lithospheric scale:

$$\Delta T = \frac{|\dot{T}|}{\dot{\epsilon}_0} = \frac{\dot{\epsilon}_0 10^{1.7}}{\epsilon_T \dot{\epsilon}_0} = \frac{50}{\epsilon_T} \approx 1000. \tag{34}$$

It is clear that these conditions are likely to be encoutered in the lithosphere which is the thermal boundary layer at the top of the convecting mantle across which a temperature drop of $\approx 1000°C$ takes place. Because the value obtained for ΔT is derived from wet olivine rheological parameters, it is therefore reasonable to conclude that localization takes place in the Earth's lithosphere because its composition (hence rheology) is dominated by olivine. This conclusion has potentially much bearing on the current assertion that it is strain localization in the Earth's lithosphere that has led to the peculiar plate kinematics observed today at the Earth's surface and that we call plate tectonics [*Zhong and Gurnis,* 1996; *Bercovici,* 1996].

Appendix A: Condition for Localization at Constant Temperature

Using (15), the grain size evolution equation (4) may be written as

$$(\dot{\bar{d}} + \dot{D}_i) = -\frac{A_2 \tau (\bar{d} + D_i)^{-m}}{\epsilon_T} (\bar{d} + D_i - d_\infty). \tag{A1}$$

We note that

$$(\bar{d} + D_i)^{-m} = \bar{d}^{-m} - m\bar{d}^{-m-1} D_i + \mathrm{O}(D_i^2), \tag{A2}$$

and, as imposed by the boundary condition,

$$\begin{aligned} \dot{\epsilon}_0 &= \frac{1}{N}\sum_{i=1}^{N} \dot{\epsilon}_i = \frac{1}{N}\sum_{i=1}^{N} A_2 \tau d_i^{-m} \\ &\approx \frac{1}{N}\sum_{i=1}^{N} A_2 \tau (\bar{d}^{-m} - m\bar{d}^{-m-1} D_i) \\ &= \frac{1}{N}\sum_{i=1}^{N} A_2 \tau \bar{d}^{-m} = A_2 \tau \bar{d}^{-m}. \end{aligned} \tag{A3}$$

Summing (A1) over all the bands gives (18):

$$\dot{\bar{d}} = -\frac{\dot{\epsilon}_0}{\epsilon_T}(\bar{d} - d_\infty). \tag{A4}$$

Combining (A1) and (18) leads to (19):

$$\dot{D}_i = -\frac{\dot{\epsilon}_0}{\epsilon_T} D_i [1 - m(1 - \frac{d_\infty}{\bar{d}})]. \tag{A5}$$

Appendix B: Condition for Transition to GSS Creep at Constant Cooling Rate

In order to express the condition for transition into GSS creep under constant cooling, let us consider the grain size evolution equation (4) when the system is in the dislocation creep regime. Combining the piezometric equation (5) to the constitutive relationship for dislocation creep (2) yields

$$d_\infty = B(\frac{A_1}{\dot{\epsilon}_0})^{\frac{p}{n}}, \tag{B1}$$

which, in turn, can be used in the mean grain size evolution equation (18).

In the case of a cooling system the piezometric grain size is varying exponentially with time, through the temperature dependence of the dislocation creep viscosity, i.e., through A_1 in (B1). This strong time dependency must be taken into account when determining the condition for transition into GSS creep. Noting that

$$\dot{d_\infty} = d_\infty \frac{Q_1 \dot{T}}{RT^2} \frac{p}{n}, \tag{B2}$$

the dimensionless form of (18) becomes

$$\dot{\bar{\delta}} = -\frac{\dot{\epsilon}_0}{\epsilon_T}[\bar{\delta}(1 + \frac{Q_1}{RT^2}\dot{T}\frac{p}{n}\frac{\epsilon_T}{\dot{\epsilon}_0}) - 1], \tag{B3}$$

where the mean grain size has been scaled according to

$$\bar{\delta} = \frac{\bar{d}}{d_\infty} \tag{B4}$$

and $\dot{T}$ is the rate of temperature change ($\dot{T} < 0$ during cooling).

For $\bar{\delta}$ to decrease toward its asymptotic ($t = \infty$) value therefore requires that the factor multiplying $\bar{\delta}$ in (B3) be negative, which implies that

$$|\dot{T}| < \frac{\dot{\epsilon}_0}{\epsilon_T}\frac{RT^2}{Q_1}\frac{n}{p}. \tag{B5}$$

Note that the asymptotic value for $\bar{\delta}$ is no longer 1 but $1/(1+\alpha)$ where,

$$\alpha = \frac{Q_1}{RT^2}\dot{T}\frac{p}{n}\frac{\epsilon_T}{\dot{\epsilon}_0}, \tag{B6}$$

and the condition for the transition from dislocation to GSS creep (13) becomes

$$\dot{\epsilon}_0^{1+mp-n} > A_1^{1+mp}B^{mn}A_2^{-n}(\frac{1}{1+\alpha})^{mn}. \tag{B7}$$

Appendix C: Condition for Localization at Constant Cooling Rate

Equation (19) can be made dimensionless by scaling the grain size perturbation, D_i, by $\bar{d}_c$,where

$$\bar{d}_c = [B(\frac{A_2}{\dot{\epsilon}_0})^p]^{\frac{1}{1+mp}}. \tag{C1}$$

This leads to

$$\dot{\Delta}_i = -\frac{\dot{\epsilon}_0}{\epsilon_T}\Delta_i[1+\kappa-m(1-\bar{\delta}^{-(mp+1)})], \tag{C2}$$

where

$$\Delta_i = \frac{D_i}{\bar{d}_c} \tag{C3}$$

$$\kappa = \frac{Q_2}{RT^2}\dot{T}\frac{\epsilon_T}{\dot{\epsilon}_0}\frac{p}{1+mp} \tag{C4}$$

$$\bar{\delta} = \frac{\bar{d}}{\bar{d}_c} \tag{C5}$$

because

$$\dot{\bar{d}}_c = \bar{d}_c\frac{Q_2}{RT^2}\dot{T}\frac{p}{1+mp}. \tag{C6}$$

The condition for localization becomes

$$\bar{d} > [\frac{m}{m-1-\kappa}B(\frac{A_2}{\dot{\epsilon}_0})^p]^{\frac{1}{1+mp}} \tag{C7}$$

or, using (27),

$$\bar{d} > (\frac{m}{m-1-\kappa})d_\infty. \tag{C8}$$

Under constant cooling conditions the dimensionless form of the equation governing the evolution of the mean grain size (18) is

$$\dot{\bar{\delta}} = -\frac{\dot{\epsilon}_0}{\epsilon_T}(\bar{\delta}[1+\kappa]-\bar{\delta}^{-mp}), \tag{C9}$$

which has the following asymptotic ($t = \infty$) solution:

$$\bar{\delta}_\infty = [\frac{1}{1+\kappa}]^{\frac{1}{1+mp}}. \tag{C10}$$

This solution satisfies the condition for localization (28) when

$$\kappa < \frac{-1}{1+m} \tag{C11}$$

or

$$|\dot{T}| > \frac{RT^2}{Q_2}\frac{\dot{\epsilon}_0}{\epsilon_T}\frac{1+mp}{p(1+m)}, \tag{C12}$$

which becomes the condition for permanent localization.

Appendix D: Condition for Localization by Grain Growth

When the grain size evolution equation is dominated by grain growth, it takes the form

$$\dot{d}_i = \frac{k}{d_i} \tag{D1}$$

or

$$\dot{\bar{d}}+\dot{D}_i = \frac{k}{\bar{d}+D_i} = \frac{k}{\bar{d}}-\frac{kD_i}{\bar{d}^2}+O(D_i^2) \approx \frac{k}{\bar{d}}-\frac{kD_i}{\bar{d}^2}. \tag{D2}$$

Summing over all bands gives the evolution equation for the mean grain size $\bar{d}$:

$$\dot{\bar{d}} = \frac{k}{\bar{d}}, \tag{D3}$$

which, combined with (D2), can be used to determined the evolution equation for D_i:

$$\dot{D}_i = -\frac{kD_i}{\bar{d}^2}. \tag{D4}$$

The only possible scaling length (or grain size) for this equation is

$$\bar{d}_s = \sqrt{\frac{-kQ_3}{R\dot{T}}}. \tag{D5}$$

Noting that

$$\dot{\bar{d}}_s = -\frac{Q_3\dot{T}}{2RT^2}\bar{d}_s, \tag{D6}$$

one can write the grain size evolution equation in the following dimensionless form:

$$\dot{\Delta}_i = -\Delta_i(\frac{k}{\bar{d}^2}-\frac{Q_3\dot{T}}{2RT^2}), \tag{D7}$$

which has an exponentially increasing solution when

$$|\dot{T}| < \frac{2kRT^2}{Q_3\bar{d}^2}. \tag{D8}$$

Acknowledgments. We are grateful to J. Fitzgerald and D. Burbidge for useful comments made during the preparation of this manuscript as well as S. Karato, G. Hirth, and an anonymous reviewer for very constructive comments.

References

Beeman, M. L., and D. L. Kohlstedt, Deformation of fine-grained aggregates of olivine plus melt at high temperatures and pressures, *J. Geophys. Res.*, *98*, 6443–6452, 1993.

Bercovici, D., Plate generation in a simple model of lithosphere-mantle flow with dynamic lubrication, *Earth Planet. Sci. Lett.*, *144*, 41-51, 1996.

De Bresser, J. H. P., C. J. Peach, J. P. J. Reijs, and C. J. Spiers, On dynamic recrystallization during solid state flow: Effects of stress and temperature, *Geophys. Res. Lett.*, *25*, 3457–3460, 1998.

Derby, B., and M. F. Ashby, On dynamic recrystallisation, *Scri. Metall.*, *21*, 879–884, 1987.

Drury, M. R., and J. D. Fitzgerald, Mantle rheology: insigths from laboratory studies of deformation and phase transition, in *The Earth's Mantle–Composition, Structure and Evolution*, edited by I. Jackson, pp. 503–559, Cambridge Univ. Press, New York, 1998.

Dutruge, G., J. Chéry, and J.-E. Hurtrez, Une approche unmérique des effets de la taille de grain sur la localization de la déformation numérique. *C. R. Acad. Sci., Ser. I*, *317*, 195–201, 1993.

Eggeler, G., and W. Blum, Coarsening of the dislocation structure after stress reduction during creep of NaCl single crystals, *Philos. Mag. A*, *44*, 1065–1084, 1981.

Furlong, K. P., Thermal-rheologic evolution of the upper mantle and the development of the San Andreas fault system, *Tectonophysics*, *223*, 149–164, 1993.

Govers, R., and M. J. R. Wortel, Initiation of asymmetric extension in continental lithosphere, *Tectonophysics*, *223*, 75–96, 1993.

Handy, M. R., The solid–state flow of polymineralic rocks, *J. Geophys. Res.*, *95*, 8647–8661, 1990.

Hirth, G., and D. L. Kohlsted, Experimental constraints on the dynamics of the partially molten upper mantle: Deformation in the diffusion creep regime, *J. Geophys. Res.*, *100*, 1981-2001, 1995a.

Hirth, G., and D. L. Kohlsted, Experimental constraints on the dynamics of the partially molten upper mantle: Deformation in the dislocation creep regime, *J. Geophys. Res.*, *100*, 15,441–15,449, 1995b.

Hopper, J. R., and W. R. Buck, The initiation of rifting at constant tectonic force: Role of diffusion creep, *J. Geophys. Res.*, *98*, 16,213–6,221, 1993.

Jin, D., S. Karato, and M. Obata, Mechanisms of shear localization in the continental lithosphere: Inference from the deformation microstructures of peridotites from the Ivrea Zone, northwestern Italy, *J. Struct. Geol.*, *20*, 195–209, 1998.

Kameyama, M., D. A. Yuen, and H. Fujimoto, The interaction of viscous heating with grain-size dependent rheology in the formation of localized slip zones, *Geophys. Res. Lett.*, *24*, 2523-2526, 1997.

Karato, S., Grain growth kinetics in olivine aggregates, *Tectonophysics*, *168*, 255–273, 1989.

Karato, S., M. Toriumi, and T. Fujii, Dynamic recrystallization of olivine single crystals during high temperature creep, *J. Geophys. Res. Lett.*, *7*, 649–652, 1980.

Karato, S., M. Toriumi, and T. Fujii, Dynamic recrystallization and high temperature rheology of olivine, In *High Pressure Research in Geophysics*, edited by S. Akimoto and M. H. Manghnani, pp. 171–189, Cent. for Acad. Press, Tokyo, 1982.

Karato, S., M. S. Paterson, and J. D. FitzGerald, Rheology of synthetic olivine aggregates: Influence of grain size and water, *J. Geophys. Res.*, *91*, 8151–8176, 1986.

Langdon, T. G., and F. A. Mohamed, The characteristics of independent and sequential creep processes, *J. Aust. Inst. Metals*, *22* 189–199, 1977.

Paterson, M. S., *Experimental Rock Deformation: The Brittle Field*, 142 pp., Springer-Verlag, New York, 1978.

Poirier, J.-P., Shear localization and shear instability in materials in the ductile field, *J. Struct. Geol.*, *2*, 135–142, 1980.

Ross, J. V., H. G. AvéLallemant, and N. L. Carter, Stress dependence of recrystallized grain–size and subgrain size in olivine, *Tectonophysics*, *70*, 39–61, 1980.

Rutter, E. H., Experimental study of the influence of stress, temperature and strain on the dynamic recrystallization of Carrara marble, *J. Geophys. Res.*, *100*, 24,651–24,663, 1995.

Rutter, E. H., and K. H. Brodie, The role of tectonic grain size reduction in the rheological stratification of the lithosphere, *Geol. Rundsch.*, *77*, 295–308, 1988.

Sakai, T., Dynamic recrystrallization of metallic materials, in *Rheology of Solids and of the Earth*, edited by S. Karato and M. Toriumi, pp. 284–307, Oxford Univ. Press, New York, 1989.

Taplin, D. M. R., G. L. Dunlop, and T. G. Langdon, Flow and failure of superplastic materials, *Annu. Rev. Mater. Sci.*, *9*, 151–189, 1979.

Tackley, P. J., Self-consistent generation of tectonic plates in three-dimensional mantle convection, *Earth Planet. Sc. Lett.*, *157*, 9–22, 1998.

Twiss, R. J., Theory and applicability of a recrystallized grain size paleopiezometer, *Pure Appl. Geophys.*, *115*, 227–244, 1977.

Urcola, J. J., and C. M. Sellars, Effect of changing strain rate on stress-strain behavior during high temperature deformation, *Acta Metall.*, *35*, 2637–2647, 1987.

Van der Wal, D., P. Chopra, M. Drury, and J. FitzGerald, Relationship between dynamically recrystallized grain size and deformation conditions in experimentally deformed olivine rocks, *Geophys. Res. Lett.*, *20*, 1479–1482, 1993.

Vissers, R. L. M., M. R. Drury, E. H. Hoogerduijn Strating, C. J. Spiers, and D. van der Wal, Mantle shear zones and their effect on lithosphere strength during continental breakup, *Tectonophysics*, *249*, 155–171, 1995.

White, S. H., M. R. Drury, S. E. Ion, and F. J. Humphreys, Large strain deformation studies using polycrystalline magnesium as a rock analog, part 1, Grain paleopiezometry in mylonite zones, *Phys. Earth Planet. Inter.*, *40*, 201–207, 1985.

Zhong, S., and M. Gurnis, Interaction of weak faults and non-Newtonian rheology produces plate tectonics in a 3D model of mantle flow, *Nature*, *383*, 245-247, 1996.

J. Braun, Research School of Earth Sciences, The Australian National University, Canberra, ACT 0200, Australia. (Jean.Braun@anu.edu.au)

J. Chéry, A. Poliakov, D. Mainprice, A. Vauchez, A. Tomassi and M. Daignières, ISTEEM, Université des Sciences et Techniques du Languedoc, Case 060, place Eugène Bataillon, 34095 Montpellier Cedex 5, France

(Received October 7, 1998; revised May 17, 1999; accepted June 8, 1999.)